Journal of Alloys and Compounds 552 (2013) 180–185

Contents lists available at SciVerse ScienceDirect

Journal of Alloys and Compounds

journal homepage: www.elsevier.com/locate/jalcom

Optimization of citrate complex combustion for synthesis of transition metal oxide nanostructures

V.M. Nair [a], R. Jose [b,*], K. Raju [a], P.R.S. Wariar [a]

[a] Dept. of Physics, University College, University of Kerala, Trivandrum 695 034, India
[b] Faculty of Industrial Sciences and Technology, Universiti Malaysia Pahang, Kuantan 26300, Malaysia

ARTICLE INFO

Article history:
Received 24 August 2012
Received in revised form 7 October 2012
Accepted 9 October 2012
Available online 23 October 2012

Keywords:
Citrate complex combustion
Transition metal oxides
Perovskites
Nanostructured transition metal oxides
Density functional theory
Optimized combustion synthesis

ABSTRACT

Combustion of citrate complex is a popular choice to synthesize nanocrystals of transition metal oxides in a single-step process. The amount of citric acid used for combustion is conventionally calculated based on the total valence of the oxidizing and reducing agents while keeping the equivalent ratio unity such that combustion energy is a maximum. This paper demonstrates by employing quantum chemical calculations that the amount of citric acid could be reduced to nearly two-third if prepared for appreciable amounts. Transition metal oxides belong to quaternary double perovskite has been synthesized as nanocrystals as examples to validate the calculations.

1. Introduction

Transition metal oxides (TMOs) are a source of abundant physical properties including high-T_c superconductivity, colossal magnetoresistance (CMR) and frustrated magnetism [1–5]. Owing to the numerous possibilities at the nanoscale, their nanostructures in various morphologies are studied extensively [6,7]. Nanostructured TMOs are frequently prepared by wet-chemical methods; i.e., by dissolving the precursors for a given composition in suitable solvents and subsequent processing to obtain a homogeneous mixture which upon annealing to produce the target material [6]. The solution combustion process, which involves rapid decomposition of a solution contains metal ions, an oxidizer and a fuel, is a popular a wet-chemical method for synthesizing a large variety of TMO nanostructures [8–10]. The combustion processes is characterized by fast heating rate and short reaction times, which make it attractive for synthesis of TMO nanostructures at relatively lower cost, simplicity, and time.

Conventionally, solution combustion process involves heating an aqueous solution containing an oxidizer (mostly metal nitrates) in the presence of a fuel (urea, for example) in a glass beaker [11,12]. However, urea decomposition process can often lead to multiphase compounds in the case of ternary or quaternary TMOs due to local differences in the metal ion concentration. This drawback has been overcome by taking advantages of coordination chemistry; i.e., by coordinating the metal ions in a chelating network thereby homogeneously distributing them and their controlled release during combustion. A number of TMO nanostructures have been synthesized using chelating agents such as polyvinyl alcohol, ethylene glycol, citric acid, ethylene diamine tetra acetic acid and so on using urea as fuel and nitrates/ammonium nitrate as oxidant [9,13,14]. Most of the above chelating agents are of higher molecular weight; and therefore, the combustion energy is not always enough to remove all the carbonaceous materials from the final product. In such cases, the combustion product needs to be further heated to remove the excess carbon or other carbonaceous materials [15]. On the other hand, chelating agent such as citric acid was demonstrated to synthesize TMO nanostructures using ammonium nitrate as oxidant in a single step, i.e., without any post combustion annealing [16–18]. During the solution refluxing, the citrate complex is formed while the solution is continuously evaporated. Upon complete evaporation, the solution becomes voluminous with enormous swelling and produces foam. The foam then undergoes spontaneous ignition triggered by the trace amounts of oxidant giving ultrafine powders of the TMO.

One of the primary questions to be addressed in the combustion of the citrate-network is the balance between the exothermic energy of combustion of the citrate complex and formation energy of the target compound. Grain growth and formation of hard agglomerates result if the combustion energy is higher than the

* Corresponding author.
E-mail address: rjose@ump.edu.my (R. Jose).

0925-8388/$ - see front matter © 2012 Elsevier B.V. All rights reserved.
http://dx.doi.org/10.1016/j.jallcom.2012.10.030

formation energy of the target compound. On the other hand, if the combustion energy is lower than the formation energy of the compound, then the final product is not expected to be single phase. The amount of citric acid for preparation of TMO compounds is routinely calculated based on the total valence of the oxidizing and reducing agents keeping the equivalent ratio unity such that the energy released is a maximum [19,20]. However, this practice neither accounts the combustion energy of the citrate complex nor the formation energy of the target material. To address this issue, we have initiated density functional theory (DFT) calculations to determine the combustion energy of a citrate chelate and applied the results to synthesize a number of transition metal oxides including binary, ternary, and quaternary compounds. Our results demonstrate that single phase ternary and quaternary compounds can be synthesized as single phase using lesser amount of citric acid than that is currently adopted. However, binary TMOs are unlikely to be synthesized using a citrate chelating network without leaving carbonaceous materials; for which urea decomposition could be a better choice.

2. Experimental details

2.1. DFT calculations

A TMO molecule with formula Ba_2LaSbO_6, a complex perovskite of considerable interest [21,22], was considered for DFT calculations and generalized the results to synthesize other compounds. Hydrogen termination was used to accommodate free valences considering the fact that the citrate combustion is carried in a boiling aqueous mixture. Geometries of citrate complexes containing Ba, La, and Sb individually or fully to produce a single molecule of Ba_2LaSbO_6 were optimized. Geometry optimizations were carries out with the use of Beck's three parameter hybrid method [23] with the Lee, Yang, and Parr (B3LYP) gradient corrected correlation functional and using the standard double-ζ quality Lanl2dz basis sets [24]. The DFT calculations were performed using Gaussian 03 program packages [25]. Harmonic frequency calculations and analysis of their IR spectra were undertaken to check the accuracy of the calculations. No imaginary frequencies were observed in the IR spectra; hence indicating that the calculated geometries are acceptable. Total energies of the complexes as well as the Ba_2LaSbO_6 molecule were obtained from thermochemical data.

2.2. Combustion synthesis of Ba_2RESbO_6 (RE = La, Ho, Yb, and Tm)

Starting materials were $Ba(NO_3)_2$, RE_2O_3, and Sb_2O_3. In a typical synthesis, aqueous solution for formation of Ba_2LaSbO_6 was prepared by dissolving stoichiometric amounts of high purity $Ba(NO_3)_2$, (99.9% CDH, India), La_2O_3 (99.9% Alfa Aesar, USA), and Sb_2O_3 (99.9%, Merck, USA). The $Ba(NO_3)_2$ was dissolved in distilled water, La_2O_3 in 0.1 N nitric acid, Sb_2O_3 in boiled tartaric acid in separate glass beakers and then mixed together in a 500 ml glass beaker. Citric acid, the amount of which was based on the results of calculation, was added to the above mixture. Addition of ammonium hydroxide triggered an exothermic reaction, which is assigned to the formation of citrate chelate as well as ammonium nitrate. Excess amounts of ammonia lead to precipitation which was further dissolved by the adding nitric acid. Table 1 shows the amount of materials used for synthesis of individual compounds synthesized in this work. The above solution containing the complex precursor mixture at neutral pH was heated using a hot plate at ~250 °C in a ventilated fume hood. The solution boils on heating and undergoes dehydration and decomposition leading to a smooth deflation with enormous swelling thereby producing foam. The foam ignited spontaneously upon complete evaporation thereby giving voluminous and fluffy product of combustion. The combustion product was flown off from the beaker to its surroundings due to the high exothermicity of reaction, which was subsequently collected by placing high purity butter papers in the combustion chamber. Temperature of the combustion flame was determined using a RTD MI-100k-type temperature controller by keeping a copper–constantan thermocouple in the combustion flame.

Table 1
The amount of materials used in a typical synthesis to generate 5 g of the Ba_2RESbO_6 (RE = La, Ho, Tm, Yb).

Materials	Ba_2LaSbO_6	Ba_2HoSbO_6	Ba_2TmSbO_6	Ba_2YbSbO_6
$Ba(NO_3)_2$ (g)	3.0241	3.0482	3.0340	3.0199
RE_2O_3 (g)	1.1010	1.1018	1.1190	1.1383
Sb_2O_3 (g)	0.8430	0.8500	0.8460	0.8420
Citric acid	4.8213	4.8713	4.8418	4.8119
HNO_3 (90%) (mL)	40	40	40	40
NH_4OH (mL)	40	40	40	40
Tartaric acid (g)	6.0564	6.0768	6.0482	6.0196
Combustion Temperature (°C)	520	530	520	530

2.3. Characterization of the combustion product

The powder obtained directly after combustion, i.e., the as-prepared powder, has been tested for (i) the chemical stability, i.e., checking whether or not any reaction occur in the as-prepared solid phase, (ii) the presence of carbonaceous materials, (iii) crystal structure, and (iv) morphology. Simultaneous thermal analyses (STA) involving differential thermal analysis (DTA) and thermo gravimetric analysis (TGA) were used to detect whether or not any solid state reaction or phase transition occur in the sample (Perkin-Elmer TG/DT thermal analyzer) in the range 30–1100 °C at a heating rate of 10 °C/min in the nitrogen atmosphere. Presence of carbonaceous materials was further checked by Fourier transform infrared spectroscopy (Nicolet-Avatar 370). To check whether the combustion product was single phase, crystal structure of the combustion product was studied using powder X-ray diffraction (XRD) technique using an X-ray Diffractometer (Model Bruker D-8) employing Nickel filtered Cu Kα radiation ($\lambda \sim 1.5406$ Å). Morphologies of the powders were determined by scanning (FESEM; Quanta 200 FEG System, FEI Company, USA) and transmission electron microscopes (TEM; Model-JEOL 2010F, operating at 200 kV).

3. Results and discussion

Fig. 1 shows the optimized geometries of adsorption complexes considered in this study as well as a single molecule of Ba_2LaSbO_6. Table 2 shows the optimized bond lengths, bond angles, total energy, and adsorption energy of the above complexes. The adsorption energies were obtained from the following relation

$$E_{Ads} = E_{(Complex)} - E_{CA} \quad (1)$$

where E_{Ads} is the adsorption energy, $E_{Complex}$ is the energy of the adsorbate complex, and E_{CA} is the energy of the citric acid. The adsorption energy of the complex is likely be derived from the exothermicity upon addition of ammonium hydroxide and external heat source during refluxing the precursor solution. Table 2 shows that energy of the Ba2LaSb–citrate complex is 50% lower than that of the sum of the energies of the component citrate complexes due to the fact that it reduces the amount of citric acid required.The energy of a single molecule of Ba_2LaSbO_6 is calculated to be -1.4647×104 eV whereas that of Ba_2LaSb–citrate is -4.4822×104 eV. i.e., formation energy of Ba_2LaSbO_6 molecule is ~75% less than the energy of the total complex thereby showing that only one-fourth of the combustion energy is utilized for formation of the compound. Remaining three-fourth of combustion energy is contributed to crystallization energy, grain growth, and dissipation. The Ba_2LaSbO_6 has a monoclinic structure with two formula units in its unit cell [21]; therefore, total energy of a unit cell should be less than -2.9294×104 eV, thereby suggesting that ~50% combustion energy contributes to grain growth and dissipation energy. Thus it turns out that reducing the combustion energy is the key to synthesize nanocrystals of TMO with controlled particle size.

Currently, the amount of citric acid for preparation of a TMOs compound is calculated based on the total valence of the oxidizing and reducing agents keeping the equivalent ratio unity such that the energy released is a maximum, following Jain et al. [19,20]. In the case of Ba_2LaSbO_6, valences of all the cations are 12 and the number of coordinating sites available is three; which suggest four citric acid molecules to synthesize one molecule of Ba_2LaSbO_6. However, the present calculations demonstrate that the amount of citric acid could be reduced to one–half than the currently adopted procedure. Also, the calculation predicts that binary TMO such as TiO_2, Nb_2O_5 are difficult to be synthesized using the citrate complex combustion as all valences of a single atom cannot be coordinated by the same citric acid molecule. Our attempts to synthesize

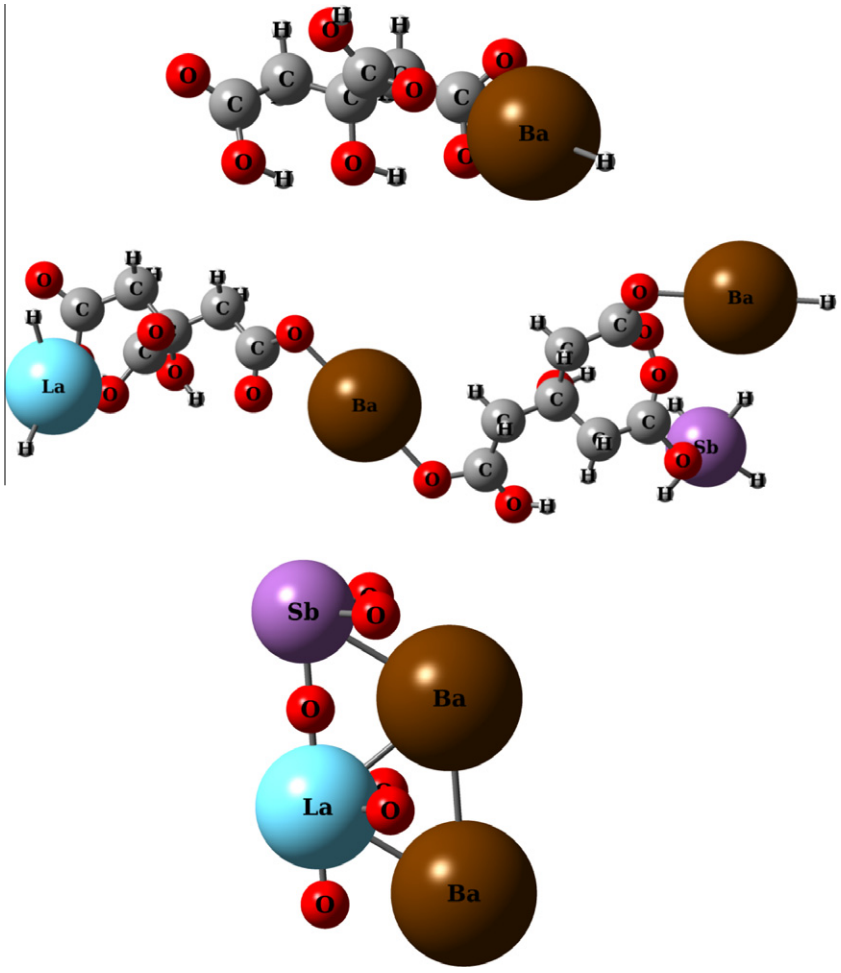

Fig. 1. Optimized structure of barium citrate, barium lanthanum antimony citrate, and barium lanthanum antimony oxide molecule at the B3LYP/lanl2dz level of DFT using Gaussian program packages.

Table 2
Bond lengths and bond angle of the adsorbate atom, total energy and adsorption energy of the citrate complex determined by the B3LYP/Lanl2dz level of DFT.

Adsorption complex	X–O bond length (Å)	X–O–C bond angle (degrees)	Total Energy (eV)	Adsorption energy of the X atom (eV)
Citric acid	–	–	-2.0674×10^4	–
Ba–citrate	2.7893	89.7435	-2.1363×10^4	6.8823×10^2
La–citrate	2.3508	136.5901	-2.0868×10^4	1.9341×10^2
Sb–citrate	2.2025	120.2288	-2.1542×10^4	8.6750×10^2
Ba_2LaSb–citrate	–	–	-4.4822×10^4	3.4235×10^3
Ba_2LaSbO_6	–	–	-1.4647×10^4	–

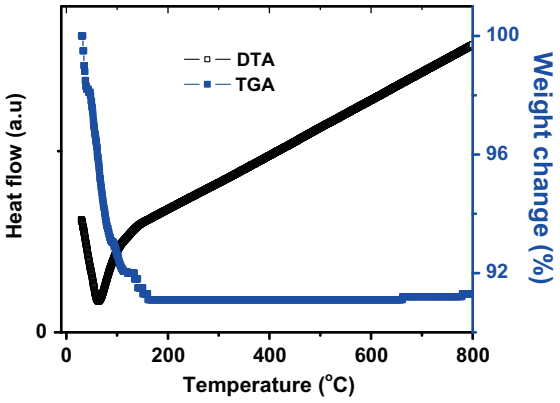

Fig. 2. Simultaneous DTA and TGA curves of the as-prepared Ba_2LaSbO_6.

binary TMOs were not successful using either when the amount of citric acid was calculated following Jain et al. or based on the present calculations. The resulting powders were always blackish because the combustion energy was not enough to remove the carbonaceous materials and required a post combustion annealing to remove them. Moreover, chelating is meant for an atomistic mixing of various atoms involved in a solid, which is not required for a binary TMO. However, we successfully synthesized ternary and quaternary compounds following the calculations. For the sake of simplicity, results of Ba_2RESbO_6 are presented here primarily because it is a quaternary TMO.

First, we determined the difference in the combustion temperature due to the change in the amount of the fuel and the oxidant using RTD MI-100 k-type temperature controller by keeping a copper–constantan thermocouple in the combustion flame. Under optimal conditions using only two-third amount of citric acid, the ignition temperature was recorded to be ~520 °C. On the other hand, the temperature of combustion was increased up to 800 °C otherwise. Excessive fuel (citric acid) and oxidant (ammonium

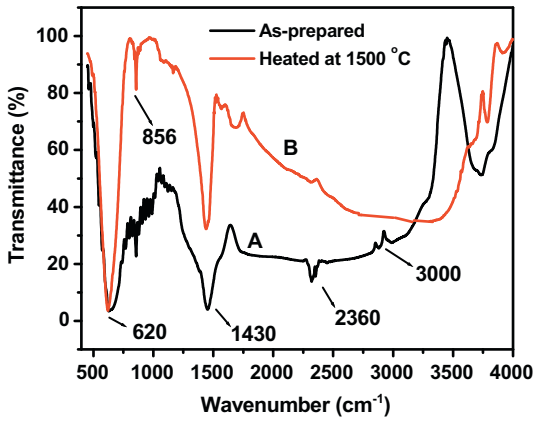

Fig. 3. FT-IR spectrum of the (A) as-prepared Ba_2LaSbO_6, and (B) that heated at 1500 °C.

nitrate) have potential risks as it lead to higher exothermicity; and therefore, the glass beaker used for the processing was often broken. Because of this higher exothermicity, the combustion process was suggested to have adverse role in its scalability in producing metal oxides on a commercial scale [16]. However, present experiment on the relationship between the combustion temperature and reaction components provide opportunities to further scale up the process to produce advanced ceramics and specialty materials on a commercial scale.

Fig. 2 shows the DTA and TGA curves of the as-prepared Ba_2LaSbO_6. The TGA showed a weight loss <5% at temperatures ~150 °C. This weight loss is attributed to the liberation of adsorbed moisture in the sample. No weight or enthalpy change occurred in the sample at higher temperatures. i.e., in the 150–1100 °C range. The usual calcination temperature of these materials are above ~1200 °C for a solid state reaction, which is further expected to be reduced due to the atomic level mixing of the reaction components during a wet chemical synthesis. This observation implies that the combustion produced a single phase material. Furthermore, a featureless STA confirms that combustion is complete with the amount of citric acid used and that no organic matter is present the sample. Similar observations were made for all the four compounds reported in this paper.

Fig. 3 shows the FT-IR spectra of the as-prepared Ba_2LaSbO_6 powder and that heated at 1500 °C. The bands in the 400–600 cm^{-1} range is generally ascribed to the asymmetric bending mode ν_4 (T_{1u}) and asymmetric stretching ν_3 (T_{1u}) mode of the SbO_6/LaO_6 octahedra [18]. The band at 858 cm^{-1} is assigned to the originally IR inactive symmetric stretching mode ν_1 (A_{1g}) of the SbO_6/LaO_6 octahedra, activated by symmetry lowering from cubic to monoclinic [21]. The broad feature in the 3000–3600 cm^{-1} region is attributed to O–H stretching of physisorbed water or from surface-adsorbed hydroxyl groups. The doublet at 2360 cm^{-1} is due to the surface adsorbed CO_2. The broad band centered at 1430 cm^{-1} is assigned to the H–O–H bending vibrations of the free or adsorbed water. The spectral noise at 3000 cm^{-1} arises from water vapor. These observations confirm the thermal analyses result that the combustion is complete and no organic matter is present in the sample. Furthermore, no shift in the IR spectral bands was observed when the samples annealed at temperatures above 1500 °C was used for FTIR measurements thereby corroborating that the combustion is complete and that no organic matter present in the as-prepared sample.

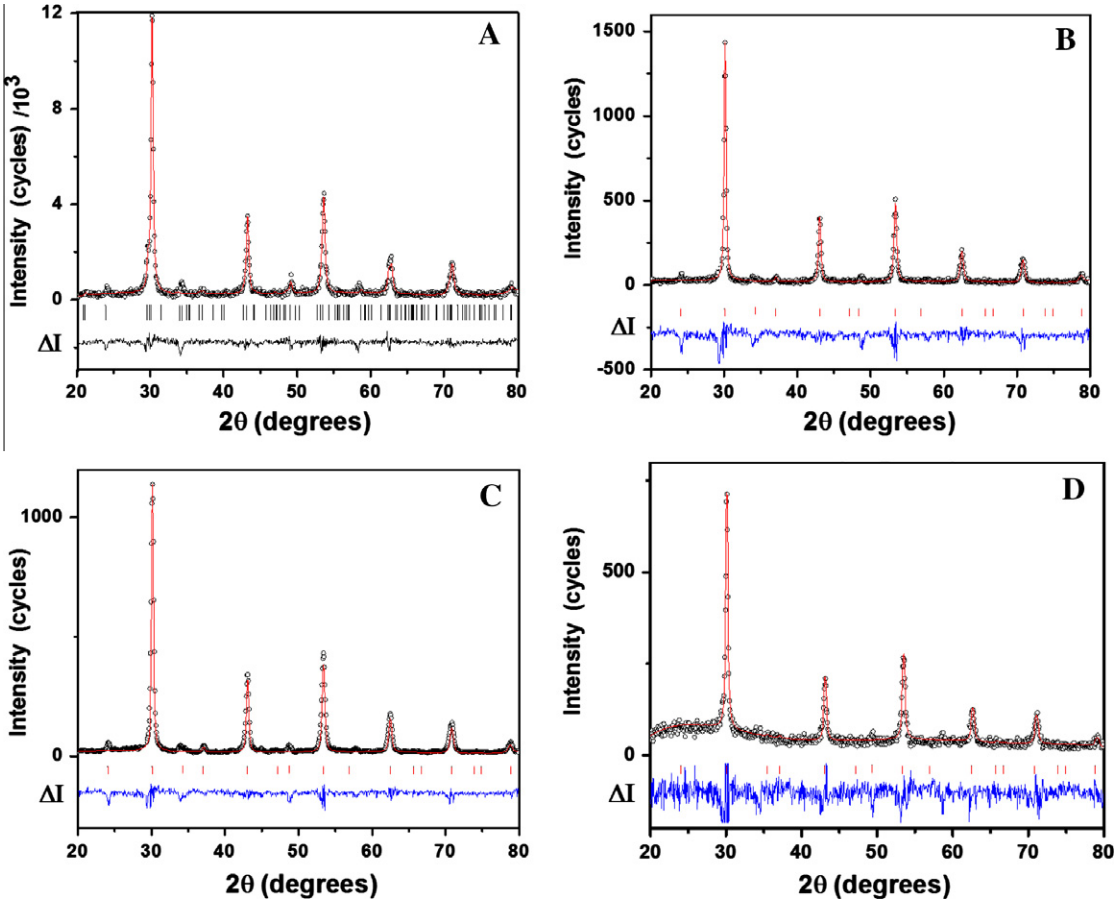

Fig. 4. XRD pattern of the as-prepared (A) Ba_2LaSbO_6, (B) Ba_2HoSbO_6, (C) Ba_2TmSbO_6, and (D) Ba_2YbSbO_6.

Table 3
Atomic and lattice parameters of Ba_2LaSbO_6 obtained by fitting the XRD patterns of the as-prepared powder using PowderCell2.3 program[26]. The residues of fitting were $R_p = 0.1525$; $R_{wp} = 0.2347$; $S = 1.43$, where the symbols have their usual meaning.

Material (Space group)	Atom	Site	x	y	z	Lattice parameter (Å)
Ba_2LaSbO_6 ($P2_1/n$)	Ba	4e	−0.00121	0.00014	0.25132	$a = 6.049$
	La	2d	0.50000	0.00000	0.00000	$b = 6.054$
	Sb	2c	0.50000	0.00000	0.50000	$c = 8.574$
	O_1	4e	0.25215	0.26492	0.00442	$\beta = 90.23°$
	O_2	4e	0.30715	−0.26642	−0.03585	
	O_3	4e	−0.02880	0.54596	0.21642	
Ba_2HoSbO_6 ($Fm\bar{3}m$)	Ba	8c	0.2500	0.2500	0.2500	$a = 8.582$
	Ho	4a	0.0000	0.0000	0.0000	
	Sb	4b	0.5000	0.0000	0.0000	
	O	24e	0.2658	0.0000	0.0000	
Ba_2TmSbO_6 ($Fm\bar{3}m$)	Ba	8c	0.2500	0.2500	0.2500	$a = 8.532$
	Tm	4a	0.0000	0.0000	0.0000	
	Sb	4b	0.0000	0.0000	0.0000	
	O	24e	0.2625	0.0000	0.0000	
Ba_2YbSbO_6 ($Fm\bar{3}m$)	Ba	8c	0.2500	0.2500	0.2500	$a = 8.462$
	Yb	4a	0.0000	0.0000	0.0000	
	Sb	4b	0.5000	0.0000	0.0000	
	O	24e	0.2625	0.0000	0.0000	

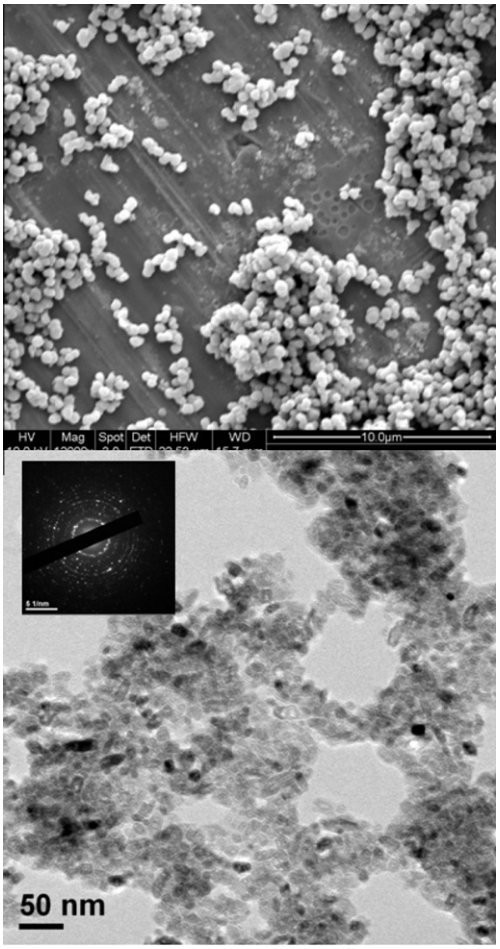

Fig. 5. SEM (top) and TEM images of the as-prepared Ba_2LaSbO_6.

Fig. 4 shows the XRD patterns of the as-prepared Ba_2RESbO_6 for 2θ between 20° and 70°. Tolerance factor calculations and experimental results show that Ba_2LaSbO_6 is monoclinic while others have a face centered cubic crystal structure [18]. The XRD patterns of the as-prepared powders were fitted to their respective crystal structures. Table 3 shows the lattice and atomic parameters of the Ba_2RESbO_6 materials. No peaks corresponding to the secondary phases were observed in the XRD patterns. i.e., the phase formation of Ba_2RESbO_6 was complete during the combustion process itself without need for an additional heating stage. In many of the combustion processes that used chelating agents such as polyvinyl alcohol, a post annealing was necessary to remove the carbonaceous materials due to the involvement of high molecular weight organic compounds. A detailed structural characterization of the materials is beyond the scope of this paper, the main purpose of which is to optimize the citrate-complex for synthesizing TMOs nanostructures.

Fig. 5 summarizes morphology of the as-prepared Ba_2LaSbO_6. The particles were observed to be uniform with an average agglomerate size of ~400 nm. The TEM studies on the powder morphology of the as-prepared Ba_2LaSbO_6 powder obtained by the combustion synthesis showed that the particles are of size 20–40 nm with a mean size of 30 nm (left panel). The ring nature of the electron diffraction pattern is indicative of the polycrystalline nature of the crystallites. One may note the particles are less agglomerated than previously reported agglomerate size [18], the origin of which is the lower combustion energy by reducing the citric acid.

4. Conclusion

In conclusion, we have shown using B3LYP/lanl2dz level of DFT and Ba_2–$LaSbO_6$ as an example that combustion energy could be reduced by controlling the amount of citric acid in the citrate complex combustion for synthesizing nanocrystals of transmission metal oxides. Experiments show that combustion flame has several hundred degree Celsius lowered temperature when only two–third amount of citric acid was used than that required by conventional process. Besides, the calculations predict that binary transition metal oxides such as TiO_2, Nb_2O_5 are difficult to be synthesized as single phase materials without leaving the carbonaceous materials using the citrate complex combustion, which were further verified by experiments. Four complex perovskites, two of which were not reported before, were synthesized as nanocrystals as single phase materials in single step processing using the results of calculations. The characterization techniques used here, such as DTA, TGA, Fourier transform infrared spectroscopy, and X-ray diffraction showed that the combustion product was single phase of the complex

perovskite. The transmission electron microscopic studies showed that the particles are less agglomerated than that produced through previously reported procedure. The reduction in agglomeration is expected to arise from the lower combustion energy by reducing the citric acid.

References

[1] Y. Tokura, N. Nagaosa, Science 288 (2000) 462.
[2] E. Dagotto, Science 309 (2005) 257.
[3] J. Orenstein, A.J. Millis, Science 288 (2000) 468.
[4] A. Sawa, Mater. Today 11 (2008) 28.
[5] H. Karunadasa, Q. Huang, B.G. Ueland, P. Schiffer, R.J. Cava, Proc. Natl. Acad. Sci. 100 (2003) 8097.
[6] S. Santra, G. Srinarayan, P. Pramanik, Trans. Indian Ceram. Soc. 69 (2010) 115.
[7] S. Ramakrishna, R. Jose, P.S. Archana, A.S. Nair, R. Balamurugan, J. Venugopal, W.E. Teo, J. Mater. Sci. 45 (2010) 6283.
[8] K. Morsi, J. Mater. Sci. 47 (2012) 68.
[9] S. Ekambaram, K.C. Patil, M. Maaza, J. Alloys Comp. 393 (2005) 81.
[10] X. Yang, Q. Li, J. Zhao, B. Li, Y. Wang, J. Alloys Comp. 475 (2009) 312.
[11] A. Chu, M. Qin, D. Rafi Ud, B. Jia, H. Lu, X. Qu, J. Alloys Comp. 530 (2012) 144.
[12] V.D. Zhuravlev, V.G. Bamburov, A.R. Beketov, L.A. Perelyaeva, I.V. Baklanova, O.V. Sivtsova, V.G. Vasil'ev, E.V. Vladimirova, V.G. Shevchenko, I.G. Grigorov, Ceram. Int. (2012), http://dx.doi.org/10.1016/j.ceramint.2012.07.078.
[13] M.A. Aghayan, M.A. Rodríguez, Mater. Sci. Eng. C 32 (2012) 2464.
[14] A. Chu, M. Qin, D. Rafi Ud, B. Jia, H. Lu, X. Qu, J. Am. Ceram. Soc. 95 (2012) 2510.
[15] A. Pathak, S. Mohapatra, S.K. Biswas, D. Dhak, N.K. Pramanik, A. Tarafdar, P. Pramanik, Am. Ceram. Soc. Bull. 83 (2004).
[16] R. Jose, A.M. John, J.K. Thomas, J. James, J. Koshy, R. Divakar, E. Mohandas, Mater. Res. Bull. 42 (2007) 1976.
[17] H.P. Kumar, C. Vijayakumar, C.N. George, S. Solomon, R. Jose, J.K. Thomas, J. Koshy, J. Alloys Comp. 458 (2008) 528.
[18] V.M. Nair, R. Jose, G.M. Anil Kumar, M.M. Yusoff, P.R.S. Wariar, J. Alloys Comp. 512 (2012) 207.
[19] S.R. Jain, K.C. Adiga, V.R. Pai Verneker, Combust. Flame 40 (1981) 71.
[20] S.R. Jain, J. Sci. Ind. Res. 62 (2003) 293.
[21] R. Jose, J. Konopka, X. Yang, A. Konopka, M. Ishikawa, J. Koshy, Appl. Phys. A. 79 (2004) 2041.
[22] P.J. Saines, B.J. Kennedy, M.M. Elcombe, J. Solid State Chem. 180 (2007) 401.
[23] A.D. Becke, Phys. Rev. A 38 (1988) 3098.
[24] C. Lee, W. Yang, R.G. Parr, Phys. Rev. B 37 (1988) 785.
[25] M.J. Frisch et al., Gaussian 03, Revision C02, Gaussian, Inc., Wallingford, CT, 2003.
[26] W. Kraus, G. Nolze, J. Appl. Crystallogr. 29 (1996) 301.